3
Literature review

Amphiphilic molecules are presented in many biological processes such as nutrient transport throughout the phospholipid bilayer of the cell membrane. In addition, some microorganisms produce these compounds as secondary metabolites that do not seem necessary for their grown and survival. They are often designated as “biosurfactants”. Such metabolites are often secreted by microorganisms either into the culture medium or are integrated into the cell wall, thus permitting them to take up hydrophobic substrates (Hausmann *et al.*, 2015).

Currently, the biosurfactants are not in direct competition with their counterpart, the synthetic surfactants. This is result of the limited availability as well as having a higher production cost (Fleurackers 2015). However, their potential to treat selectively minerals of low grade, achieving high recoveries (Khoshdast *et al.,* 2011) and in addition replacing a synthetic compound by an ecofriendly one, may justify its production. In the following pages, there is a brief review about what are biosurfactants and how they are classified and extracted. Following, it focuses about the biology of the bacteria *Rhodoccocus opacus* as well as what kind of biosurfactans are produced by this genus. Finally, there is a compilation of bioflotation studies using *R. opacus* as a biocollector reagent.

3.1.
Biosurfactants and classification

Surfactants are amphiphilic molecules whose main characteristic is their affinity for interfaces. These surface active substances have a polar head, formed by a polar chemical group, and an apolar tail, usually formed by a hydrocarbon chain. In general, synthetic surfactants produced from petroleum feedstock are used in food, mining, cosmetic, and pharmaceutical industries as emulsifiers, lubricants, stabilizers, wetting agents, etc. (Banat *et al.*, 2000; Mukherjee *et al.*, 2006). However, since they are harmful to the environment, the

PUC-Rio - Certificação Digital Nº 1421964/CA

use of more efficient and ecofriendly surfactants is a necessity (Dhanarajan *et al.*, 2014). Biosurfactants are microbial surface-active compounds, synthetized extracellulary or as part of the cell membrane, of structurally diverse molecules produced by different microorganisms and are mainly classified by their chemical structure and their microbial origin. They are made up of a hydrophilic moiety, comprising an acid, peptide cations, or anions, mono-, di-, or polysaccharides, and a hydrophobic moiety of unsaturated or saturated hydrocarbon chains or fatty acids (Mulligan *et al.,* 2014).

Regarding to their typology, biosurfactants are classified into many groups, since they are produced from wide variety of microorganisms and have very different chemical structures (Ron and Rosenberg, 2001). The major classes of biosurfactants include glycolipids, lipopeptides and lipoproteins, fatty acids, phospholipids and neutral lipids, polymeric surfactants, and particulate surfactants (Desai and Banat, 1997). Fig.3-1 shows their classification.

PUC-Rio - Certificação Digital Nº 1421964/CA

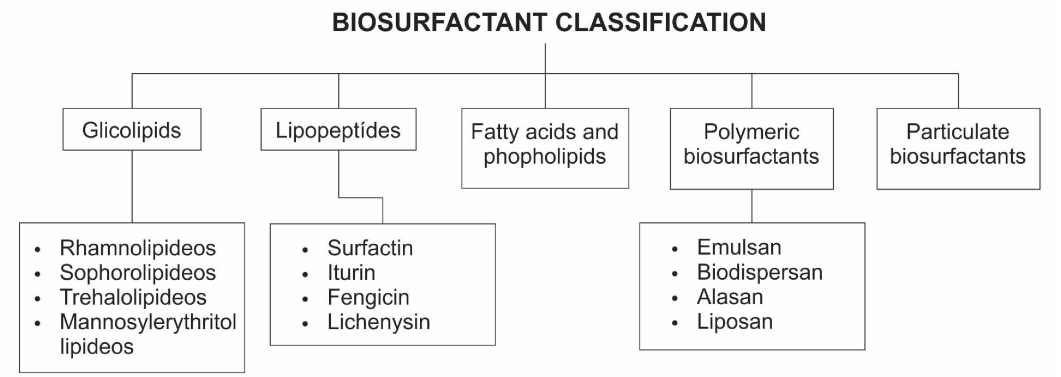

Figure 3-1: Classification of biosurfactants (adapted from Ron and Rosenberg, 2001).

3.1.1. Glycolipids

Glycolipids are carbohydrates (hydrophilic moiety) linked with long-chain aliphatic acids or hydroxy aliphatic acids (hydrophobic moiety). The linkage is by means of either ether or an ester group (Dhanarajan *et al.,* 2014). The most studied glycolipids are rhamnolipids, sophorolipids, and trehalolipids (Desai and Banat, 1997).

3.1.1.1. Rhamnolipids

They are extracellular biosurfactants produced by *Pseudomonas aureginosa*. It can produce up to 100 g/L of rhamnolipids, and hence, its cost becomes competitive against the production cost of synthetic surfactants (Maier et al. 2000). However, this bacteria is considered as pathogenic opportunistic organism (Balcht *et al.*, 1994) and therefore one of the main challenges currently faced in the area of rhamnolipid production is the need for a nonpathogenic alternative to *Pseudomonas aeruginosa* that can be used on an industrial scale (Marchant et al. 2015).

3.1.1.2. Sophorolipids

They are largely produced by yeasts, mainly *Candida sp*.; they are composed of a disaccharide sophorose, β-glycosidically linked to a long chain hydroxy fatty acid. (Dhanarajan *et al.*, 2014). The strain Candida bombicola ATCC 22214 can produce over 400 g/L sophorolipids and currently is used for commercial production and applications (Pekin *et al.*, 2005). Structurally, the sophorolipids also have two major domains, like any other biosurfactant: (1) hydrophobic domain and (2) hydrophilic domain; the hydrophobic part of the sophorolipids contains a terminal or subterminal hydroxylated fatty acid, which is linked to sophorose through β-glycoside linkage (Morya *et al.*, 2014).

3.1.1.3. Trehalolipids

Different types of trehalolipids are known to be produced by several microorganisms, including the genera of *Mycobacterium, Rhodococcus, Arthrobacter, Nocardia,* and *Gordonia*; among the trehalolipids, the trehalose esters produced by *Rhodococcus erythropolis* have been studied most extensively (Dhanarajan *et al.*, 2014). Fig. 3-2 shows the chemical structure of a generic trehalolipid.

PUC-Rio - Certificação Digital Nº 1421964/CA

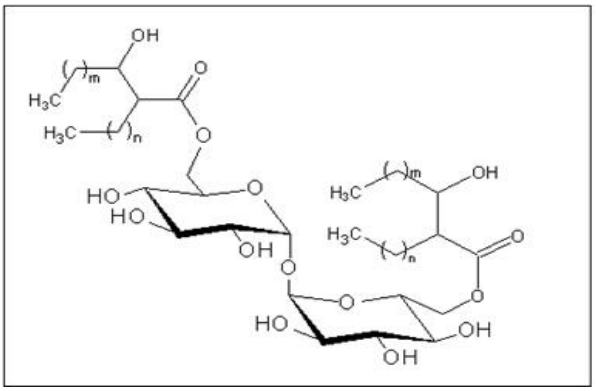

Figure 3-2: Chemical structure of a generic trehalolipid (Lang and Philp, 1998).

3.1.2. Lipopeptides

They consist of short linear chains or cyclic structures of amino acids, linked to a fatty acid via ester or amide bonds or both (Dhanarajan *et al.,* 2014). Lipopeptides contain rare and modified amino acids, which are not used for ribosomal protein synthesis (Sen, 2010). For instance, the aminoacid leucine is find in the surfactin as a D isomer, however the proteins are only composed of L isomers.

3.1.2.1. Surfactin

It is a lipopeptide-type biosurfactant that is generated by the gram-positive, endospore-producing, microorganism, *Bacillus subtilis* (Chen *et al.,* 2015). The cyclic lipopeptide surfactin consists of 3-hydroxy-13-methyl-tetradecanoic acid linked to the N-terminal amine of a heptapeptide moiety with the carboxy terminal end of the peptide being further esterified to the hydroxyl group of the fatty acid (Sen, 2010).

3.1.2.2. Lichenysin

They are lipopeptide biosurfactants produced by *B. licheniformis* and are named lichenysin A, B, C, D, G, and surfactant BL86 with regard to the producing strains; Lichenysin A was reported to exhibit critical micelle concentration (CMC) of 12 mg/L, which is around one-half of the CMC of surfactin, 25 mg/L (Dhanarajan *et al.,* 2014). Structurally resembles surfactin from *Bacillus subtilis*; the main

PUC-Rio - Certificação Digital Nº 1421964/CA

difference is the presence of a glutaminyl residue in the peptide sequence (Grangemard *et al.,* 2001).

3.1.3. Fatty acids and phospholipids

Various bacteria and yeasts are able to secrete surface active fatty acids and phospholipids when grown on hydrocarbons. Lipids can be minor components of a cell or excreted into the medium facilitating efficient product recovery (Dhanarajan *et al.,* 2014).

3.1.4. Polymeric biosurfactants

Polymeric biosurfactants do not necessarily reduce superficial tension, but they effectively reduce the interfacial tension between immiscible liquids and form stable emulsions. The most studied polymeric biosurfactants are emulsan and liposan, which is an effective emulsifier produced by *Candida lipolytica* capable of forming stable oil-in-water emulsions with a variety of commercial vegetable oils (Dhanarajan *et al.,* 2014).

3.1.5. Particulate biosurfactants

They are extracellular vesicles that help in hydrocarbon uptake by cells and microbial cells with surface active properties are referred to as particulate biosurfactants (Syldatk *et al.,* 2010). For instance, *Acinetobacter sp*. HO1-N produce extracellular membrane vesicles with 20–50 nm diameter and a buoyant density of 1.158 g/cm^3; they are rich in phospholipids and lipopolysaccharides, exhibiting good emulsification activity (Muthusamy *et al.,* 2008).

PUC-Rio - Certificação Digital Nº 1421964/CA

3.2.
Characteristics of Microbial Amphiphiles

3.2.1.
Surface and interface activity

Surfactin and lichenysin are the most powerful biosurfactants in reducing superficial tension at low CMC values (Dhanarajan *et al.,* 2014). Lichenysin A, a lipopeptide from *B. licheniformis*, can reduce the superficial tension of water from 72 to 28 mN/m at a CMC as low as 12 mg/L (Yakimov *et al.*, 1995). Surfactin from *B. subtilis* was reported to lower the superficial tension of water to 27 mN/m, with CMC of 25 mg/L, and interfacial tension of water/hexadecane to 1 mN/m (Cooper et al. 1981). A biosurfactant from *P. aeruginosa* isolated from the formation water of petroleum reservoir was reported to lower the superficial tension of water from 71.2 to 22.56 mN/m (Xia *et al.,* 2011). A trehalolipid from *R. erythropolis* decreased the interfacial tension of water/hexadecane to less than 1 mN/m and superficial tension of water to 26 mN/m with CMC of 15 mg/L (Lang and Philp, 1998). In addition, biosurfactants are capable of stabilizing and destabilizing the emulsion, hence widely used in dairy, food, and cosmetic industries. While low–molecular weight biosurfactants behave as efficient surface and interfacial active agents, high-molecular weight biosurfactants are effective in forming stable emulsions (Dhanarajan *et al.,* 2014).

3.2.2.
Temperature, pH, and ionic strength tolerance

The stability of biosurfactants at extremes of pH, temperature, and salinity is one of their unique properties that lead them to find countless industrial and environmental applications (Dhanarajan *et al.,* 2014). Surfactin exhibited good surface activity at a temperature of 100°C, over the pH range of 5–12, and up to 20% NaCl and 0.5% $CaCl_2$ (Gong *et al.,* 2009). Sophorolipids from *Candida bombicola* showed unhindered surface activity after 2 h incubation in boiling water, over a broad pH range of 2–10 and up to 20% NaCl (Daverey and Pakshirajan, 2010).

PUC-Rio - Certificação Digital Nº 1421964/CA

3.2.3.
Low toxicity

It was examined the toxicity of surfactin from *B. subtilis* in adult Sprague–Dawley rats for 28 days. Rats survived even with a high dose of surfactin (2 g/kg), and the no-observed-adverse-effect-level of surfactin was found to be 500 mg/kg (Hwang *et al.*, 2009). A glycolipid biosurfactant from *Rhodococcus ruber* was examined for its acute toxicity against outbred male albino mice. No effect on central nervous system or weight loss was found during the 14-day observation (Kuyukina *et al.*, 2007). Few other reports have also compared the toxicity of biosurfactants and chemical counterparts, indicating the low toxicity of biosurfactants (Dehghan-Noudeh *et al.*, 2005; Edwards *et al.*, 2003; Hirata *et al.*, 2009; Poremba *et al.*, 1991).

3.2.4.
Biodegradability

As the concern about the environment is increasing, easily biodegradable microbial surfactants are preferred over the synthetic surfactants for environmental applications (Nitschke and Costa, 2007). It was examined the biodegradability of rhamnolipids by incubating it in black loamy soil and red sandy soil for 1 week. The degradation rate was slow initially, but 92% of rhamnolipid was found to be mineralized in both kinds of soil at the end of the week (Pei *et al.*, 2009).

PUC-Rio - Certificação Digital Nº 1421964/CA

3.3.
Biology of *Rhodococcus*

The genus *Rhodococcus* belongs to the suborder Corynebacterineae, a distinctive lineage within the phylum Actinobacteria (Gürtler *et al.*, 2004). In addition, it is a chemoorganotrophic organism with a high hydrophobicity (Mesquita *et al.*, 2003). *The Rhodococcus* genus may be naturally present in contaminated environments and it is a promising candidate for bioremediation because of its capacity to degrade substituted hydrocarbons (Bell *et al.*, 1998). Morphologically, it is characterized by its mycelial grown with fragmentation into rod-shaped or coccoid elements (Rehfuss *et al.*, 2005).

Even though, *Rhodococcus opacus* is a gram positive bacteria, its cellular wall is covered with a monolayer of mycolic acids (Neu 1996). The mycolates form the basis of a second hydrophobic permeability barrier outside of the plasma membrane. This structure is analogous to the outer membranes of Gram-negative bacteria but is chemically and structurally distinct, most notably the defining feature of the permeability barrier is not a bilayer but the monolayer of bound mycolates (Sutcliffe et al. 2010). Figure 3-3 shows the model, it can be seen that the permeability barrier confers the hydrophobicity to the bacteria; in addition, it may facilitate the intake of apolar substrates such as hydrocarbons (Carvalho *et al.*, 2009). Fig. 3-3 shows the components of the *Rhodococci* cellular wall, note the presence of mycolic acids and dimycolates in the outer layer.

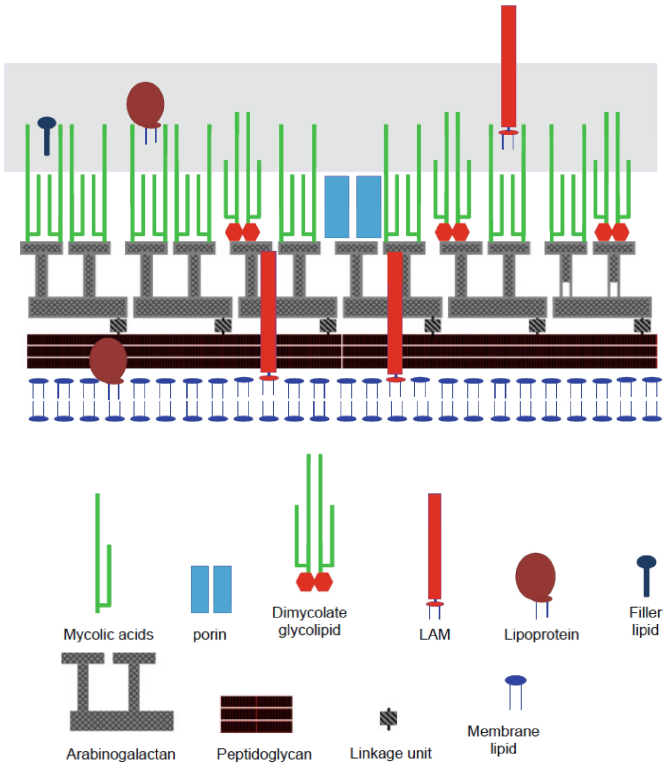

Figure 3-3: Organization of the rhodococcal cell envelope (Minnikin 1991).

3.4. *Rhodococcus´* Biosurfactants

The biosurfactants produced by the genera *Rhodococci* are predominantly cell-bound glycolipids containing trehalose as the polar head (Kuyukina *et al.*,

PUC-Rio - Certificação Digital Nº 1421964/CA

2010). Most of the research has been done on trehalolipid surfactants formed by *R. erythropolis* (Lang and Philp, 1998).

3.4.1. Structures and Physicochemical Properties

Unlike synthetic surfactants having relatively simple chemical structure, biosurfactants are usually quite complex molecules. Therefore, their physicochemical properties are more complex compared to synthetic surfactants (Kuyukina *et al.,* 2010). Trehalolipids are produced by members of closely related actinobacterial genera, including *Rhodococcus*, *Nocardia*, *Corynebacterium, Gordonia*, *Mycobacterium*, *Tsukamurella*, and *Arthrobacter*. Trehalolipids from *rhodococci* are characterized by high structural diversity, and they often occur as a complex mixture, the composition of which varies depending on strain physiology and growth conditions (Kuyukina *et al.,* 2010).

Additionally, it was observed that they lowered the surface tension of water from 72 mN/m to values between 19 and 43 mN/m and the interfacial tension of water/n-hexadecane system from 43 mN/m to values between 0.02 and 15 mN/m (Ivshina *et al.,* 1998; Philp *et al.,* 2002; Marqués *et al.,* 2009; Tokumoto *et al.,* 2009).

3.4.2. Biosynthesis and Recovery

Metabolic pathways involved in trehalolipid synthesis in *Rhodococcus* were reviewed (Lang and Philp, 1998). It seems that the trehalose moiety and the fatty (mycolic) acid moiety of trehalolipid molecules are synthesized independently and are subsequently etherified. The recovery and concentration of biosurfactants from the fermentation broth largely determine their production cost (Kuyukina et al. 2010). Often, low concentration and the amphiphilic nature of microbial surfactants limit their recovery (Desai and Banat, 1997).

Various techniques are used for biosurfactant isolation include high-speed centrifugation, dialysis and ultrafiltration, acid and salt precipitation, solvent extraction and adsorption chromatography (Bryant 1990; Desai and Banat 1997). A

PUC-Rio - Certificação Digital Nº 1421964/CA

summary of the isolation techniquesis shown in Fig. 3-4. However, surfactants produced by *rhodococci* under unrestricted growth conditions are predominantly cell-associated trehalolipids, which can be effectively isolated only by the organic solvent extraction (Lang and Philp 1998). A wide variety of organic solvents, for example, methanol, ethanol, diethyl ether, pentane, acetone, chloroform, and dichloromethane have been used, either singly or in combination (Desai and Banat 1997).

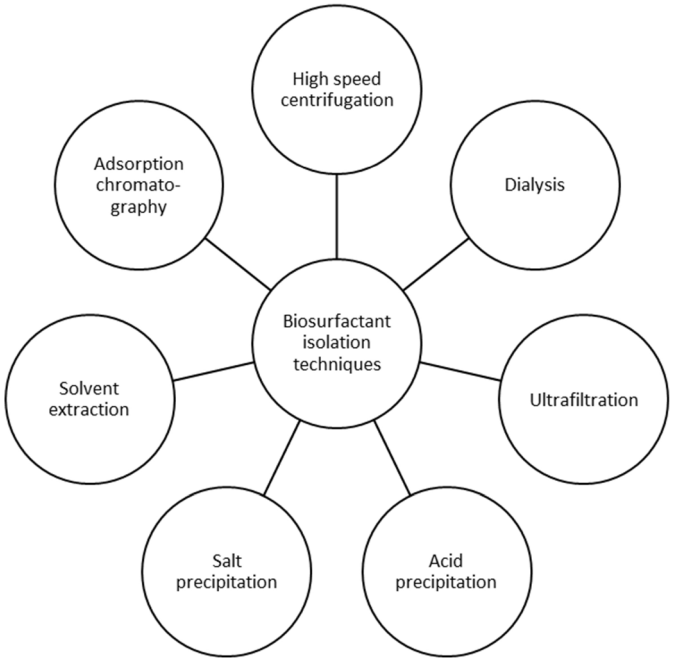

Figure 3-4: Biosurfactant isolation techniques adapted from Mulligan et al., 2009.

3.4.3. Physiological Roles and Biological Activity

Bacteria of the genus *Rhodococcus* are able to utilize aliphatic and aromatic hydrocarbons of extremely low water solubility as carbon and energy sources (Kuyukina *et al.*, 2010). The role of biosurfactants is related to the low water-solubility of n-alkanes as growth substrates and is determined by the ability to reduce interfacial tension between hydrocarbons and an aqueous phase (Ron and Rosenberg 2001). Although many bacteria can assimilate hydrophobic substrates in solubilized or emulsified forms, the hydrocarbon uptake by *Rhodococcus* occurs by direct cell contact with large oil drops (Lang and Philp 1998).

PUC-Rio - Certificação Digital Nº 1421964/CA

Cell-associated biosurfactants promote the adhesion of *rhodococcal* cells not only to liquid hydrocarbons, but also to hydrophobic solid surfaces (Neu 1996), allowing effective cell colonization and direct uptake from sorbed/crystalline hydrocarbons (Whyte et al. 1999). In addition, trehalose mycolates along with other cell-wall lipids are involved in cellular tolerance to antibiotics and organic solvents (Kuyukina *et al.,* 2000; Sokolovska *et al.,* 2003; Nguyen *et al.,* 2005), as well as to physical factors, for example, high temperature and desiccation (Sung *et al.,* 2004; LeBlanc *et al.,* 2008).

3.5. Ethanol extraction processes

Ethanol is a clear, colorless liquid (at 25 °C and 1 atm) characterized as GRS (Generally Recognized as Safe) by the FDA (Mustafa *et al.,* 2012). Its affinity for polar and apolar substances because of its chemical structure, in addition, with its relatively low environmental impact (Hill *et al.,* 2006; Kim and Dale 2005) makes it a good alternative in the recovery of organic compounds such as lipids, vitamins or proteins.

3.5.1. Pressurized Hot Ethanol Extraction of Carotenoids from Carrot By-Products

Approximately 600 unique carotenoids can be found in plant species, as well as select species of algae and fungi (Eugster 1995). Health scientists have identified a wide range of functions, from optical enhancement within the eye to immunomodulatory and antioxidant functions (Hammond *et al.,* 2001). Mustafa *et al.,* 2012 extracted carotenoids from carrots regarded as by-products due to strict market policies. Pressurized liquid extraction (PLE) utilizes conventional solvents at elevated temperatures and pressure, and it requires less solvent and shorter extraction times (Saldaña *et al.,* 2006). All the extraction experiments were conducted using an Accelerated Solvent Extraction (ASE-200™) equipment from Dionex Corp. (Salt Lake City, UT, USA). The results are shown in Fig. 3-5.

PUC-Rio - Certificação Digital Nº 1421964/CA

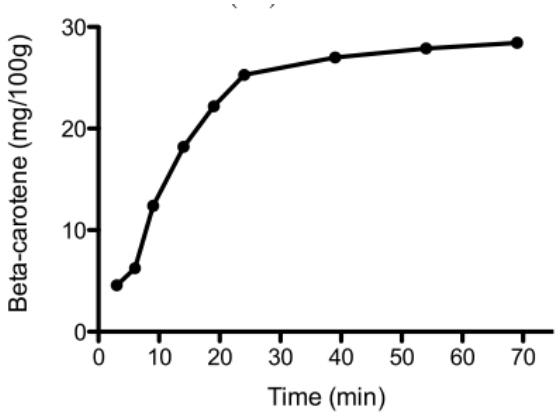

Figure 3-5: Extraction curve showing cumulative concentrations of β-carotenes (Mustafa et al., 2012).

3.5.2. Ethanol–water extraction of lignans from flaxseed

The lignans are a group of polyphenolic compounds found in plants. Secoisolariciresinol diglycoside (SDG), a kind of phytoestrogen, is the main component of flaxseed lignans (Prasad 2005). Previous researches indicated that SDG could prevent mammary, colonic, and prostate cancer (Ingram *et al.*, 1997). As can be seen from Fig. 3-6, the acquired ratio of lignans as a function of ethanol concentration follows a parabola shape. The acquired ratio of lignans increased with increasing of the ethanol proportion in the extraction medium up to 70% and then began to decline with the further increase of ethanol proportion in the extraction medium (Zhang *et al.*, 2007).

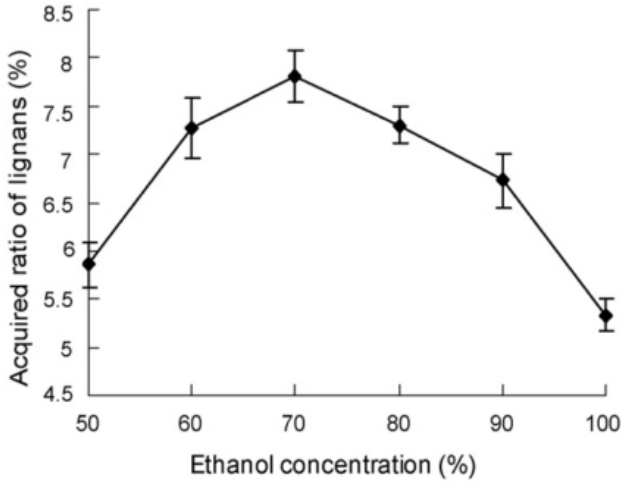

Figure 3-6: Influence of ethanol concentration on the acquired ratio of lignans of flaxseed (Zhang et al., 2007).

PUC-Rio - Certificação Digital Nº 1421964/CA

3.6. Electric double layer modeling and thermodynamic approach

The theory of the electrical double layer play a significant role in the mineral flotation chemistry because it helps to explain the mechanism by which the reagent is attached to the mineral surface. Most solid surfaces in contact with water or an aqueous solution will be found to develop some type of electrical charge. The magnitude of that charge may be quite small or very large, but it will almost always exist (Myers 1999). Surface charges cause an electric field. This electric field attracts counter ions. The layer of surface charges and counter ions is called "electric double layer" (Butt *et al.,* 2003).

An important equation that shows the relationship between the concentration of the potential determining ions and the surface potential is given by the Nernst equation. Where ψ_0 is the surface potential, R is universal gas constant, F is the faraday constant, c is the concentration of the potential determining ions and c_{zp} is the ion concentration at the point of zero charge (Hiemenz *et al.*, 1997).

$$\cdot_{0} \mathrm{X} 2.303 \frac{RT}{F} \log \frac{c}{c_{zp}} \tag{3-1}$$

Assuming that the potential determining ions are the hydrogen ions H^+. It is possible to derive a relationship between the pH and the surface potential.

$$\cdot_{0} \mathrm{X} 2.303 \frac{RT}{F} fPZC \mathrm{Z}\, pH A \tag{3-2}$$

3.6.1. Helmholtz model

In the simplest model of an electric double layer, the counter ions bind directly to the surface and neutralize the surface charges much like in a plate capacitor (Butt *et al.,* 2003). Therefore, the potential drop in the Helmholtz model can be derived based on the assumption the system behaves like a plate capacitor as Eq. 3-3 shows. Where $\Delta\psi$ is the potential variation, δ is the distance between the

PUC-Rio - Certificação Digital Nº 1421964/CA

opposite charges, σ is the charge density per area, ε_r is the dielectric constant of water (its bulk value around 80) and ε_0 is the vacuum permittivity (Hiemenz *et al.*, 1997).

$$\frac{\zeta \cdot}{\text{¢}} \text{X} \frac{\pm}{£_r £_0} \tag{3-3}$$

In addition, the charge density can be estimated based on the Grahame equation (Butt *et al.,* 2003). For low potentials, it takes the simplified form showed in Eq. 3-4.

$$\pm \text{X} \frac{£_r £_0 \cdot_0}{\text{a}_D} \tag{3-4}$$

Where a_D is the Debye length, defined as the distance at which the potential is reduced to 0.37 of the surface potential (Butt *et al.,* 2003). For a monovalent ion it takes the form showed in Eq. 3-5. The term k_B is the Boltzman constant.

$$\text{a}_D \text{X} \frac{1}{\sqrt{\frac{2c_0 e}{£_r £_0 k_B T}}} \tag{3-5}$$

3.6.2. Gouy and Chapman model

One of the fails of the Helmholtz capacitor model is that it does not take into account the thermal motion of the ions. Thermal fluctuations tend to drive the counterions away form the surface. They lead to the formation of a diffuse layer, which is more extended than a molecular layer (Butt *et al.,* 2003). Fig. 3-7 shows the two models.

PUC-Rio - Certificação Digital Nº 1421964/CA

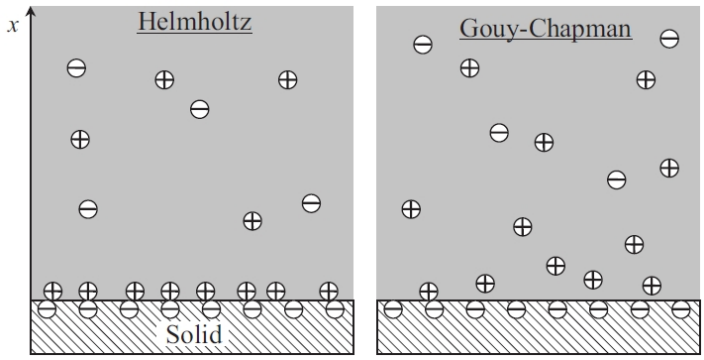

Figure 3-7: Helmholtz and Gouy–Chapman model of the electric double layer (But et al., 2003).

In order to derivate an expression for the potential distribution, it is necessary to define two important equations. The first one, known as the Poison equation, relates the potential and charge density per volume.

$$\nabla^2 \cdot = \frac{\partial^2 \cdot}{\partial x^2} + \frac{\partial^2 \cdot}{\partial y^2} + \frac{\partial^2 \cdot}{\partial z^2} = -\frac{\rho_e}{\varepsilon\varepsilon_0} \tag{3-6}$$

In order to solve the Poison equation, it is mandatory to know the charge distribution. This relation is given by the Boltzman equation, where c_0 is the concentration of the electrolyte.

$$\rho_e = -c_0 e^{-\frac{e \cdot f(x,y,z)}{k_B T}} + c_0 e^{\frac{e \cdot f(x,y,z)}{k_B T}} \tag{3-7}$$

Finally, substituting Eq. 6 into Eq. 5, the Poison-Boltzman equation is obtained. For planar surfaces and low potential, it has an analytical solution, as shown in Eq. 7. Where a_D is the Debye length.

$$\cdot = \cdot_0 e^{-\frac{x}{a_D}} \tag{3-8}$$

In the treatment of the diffuse electric double layer, several assumptions were made which lead to imperfections (Quesada-Pérez *et al.*, 2003):

- The finite size of the ions was neglected.

PUC-Rio - Certificação Digital Nº 1421964/CA

- Ions in solution were considered as a continuous charge distribution.

- All non-Coulombic interactions were disregarded.

- The solvent is supposed to be continuous and the permittivity of the medium constant.

- Surfaces are assumed to be flat on the molecular scale.

3.6.3. Stern layer

Stern combined the ideas of Helmholtz and that of a diffuse layer (Quesada-Pérez *et al.,* 2003). The assumption that ions have no volume is acceptable for the bulk region of dilute solutions, but real ions cannot be drawn toward charged surfaces without crowding becoming a .problem. At the inner edge of the diffuse part of the double layer some sort of saturation limit must be approached (Hiemenz *et al.,* 1997). Fig. 3-8 shows the electric double layer model including the Stern layer.

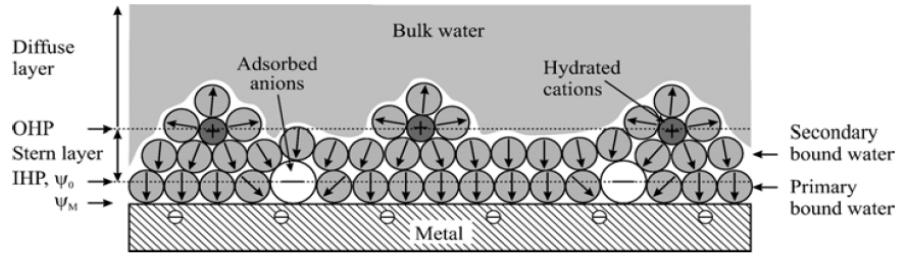

Figure 3-8: Stern layer at a metal surface. Where the inner (IHP) and outer (OHP) Helmholtz planes are indicated (Butt et al., 2003).

The complete mathematical expression for the double layer incorporating the Stern layer is quite complex (Myers 1999). However, because of some strong ion adsorption at the surface, the actual electrostatic potential-energy curve may show a break at the Stern layer. Considering that the Stern layer thickness must be really small, it is valid the assumption that the potential is linear in this region and can be adjusted to a plate capacitor potential drop model. The potential profile of an electric layer with specific adsorption is shown at Fig. 3-9.

PUC-Rio - Certificação Digital Nº 1421964/CA

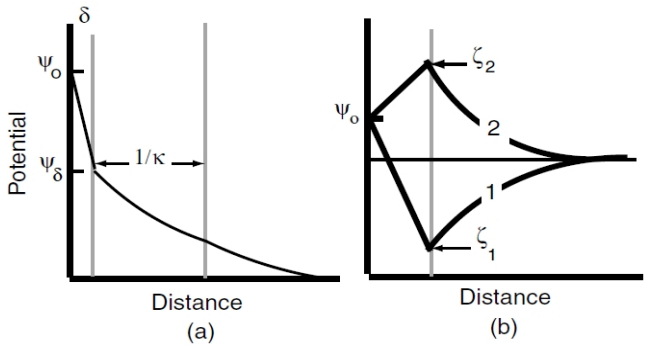

Figure 3-9: Breaks at the Stern layer (a); additional specific adsorption processes may further alter the curve resulting in an incremental or reversal potential (b) (Myers 1999).

In addition, the constraint that the charge density on the surface remains constant under all conditions is vital for the modelling (Myers 1999). In reality, as the environment of an interface is altered by two opposed charged approaching each other, there is a potential overlapping resulting in the neutralization of both.

3.6.4. Gibbs free energy of the electric double layer

The estimation is based on assumption that only the diffuse layer is relevant, however the formalism is, however, applicable to other double layers as well (But *et al.*, 2013). In order to calculate the Gibbs free energy of a Gouy–Chapman layer the electric double layer formation is split in three steps (Chan *et al.*, 1983).

- First, the uncharged colloidal particle is brought into an infinitely large solution.

- The counterions are been brought to the surface.

- On a third step the counterions are released from the surface.

Summing up all contributions, the total Gibbs free energy of the diffuse double layer per unit area is shown in Eq. 3-9; where ψ_0 is the surface potential and σ is the charge density:

$$\zeta G \, XZ\pm \cdot {}_0 \Gamma \, {}^{\pm}_{0} \cdot {}_0 'd\pm ' \qquad (3\text{-}9)$$

PUC-Rio - Certificação Digital Nº 1421964/CA

For low potentials, it is simplified to the expression shown in Eq. 3-10. The Gibbs free energy of an electric double layer must be negative because it forms spontaneously. Roughly, it increases in proportion to the square of the surface potential (Butt *et al.*, 2003).

$$\zeta G \mathrm{XZ}\frac{1}{2}\pm \cdot {}_{0} \tag{3-10}$$

3.7. Hematite flotation studies using synthetic surfactants

In order to compare the efficiency of the biosurfactants against the synthetic ones, it is necessary to have base line. Flotation tests of hematite and quartz using C12 amine, sodium oleate and sodium dodecyl sulfate were carried out in a hallimond tube using a fraction size of -150 +63 um (Vidyadhar *et al.,* 2014). The results are presented in the Fig. 3-10.

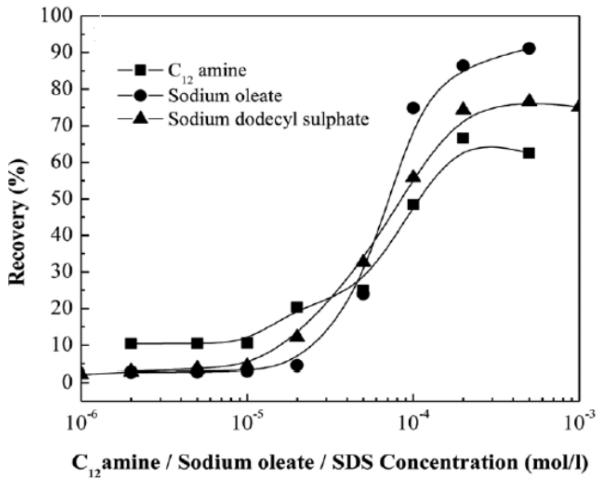

Figure 3-10: Floatability of hematite as a function of SDS, sodium oleate and C12 amine concentration at neutral pH (Vidyadhar et al. 2014).

The effect of pH is shown in Table 3-1. The hematite floatability with anionic sodium oleate increases with the increase of pH around 6.0, and thereafter, the recovery gets relatively subdued. These results show that maximum flotation recovery of about 95% is attained at highly acidic pH between 2 and 3, with anionic sodium dodecyl sulfate collector and the recovery decrements considerably with the increase of pH. In addition, it was studied the flotation of hematite using C6-C18 saturated fatty acids (Quast, 2006). It can be seen a correlation between the

PUC-Rio - Certificação Digital Nº 1421964/CA

carbon number and the hematite recovery, the fatty acids which show optimum results are between 8 and 12 chain carbon.

Table 3-1: Maximum hematite recoveries using C6-C18 saturated fatty acids as collectors at concentrations of 1 kg/t (adapted from Quast 2006)

Collector	pH	Recovery (%)
Octanoic acid	2-8	96
Decanoic acid	2-8	97
Dodecanoic acid	10-12	98
Tetradecanoic acid	6-8	50
Hexadecanoic acid	2-12	20
Octadecanoic acid	2-12	18

3.8. Mineral flotation studies using *Rhodococcus opacus* as reagent

3.8.1. Surface tension and foam formation

Due to its hydrophobic outer layer, *Rhodococcus opacus* has affinity for the interface air-water. This is supported by surface tension measurements as it is shown in Fig. 3-11 (a), where the surface tension of water decreases as the biomass concentration rises. However this behavior have a limit, after a certain concentration (in the case of *Rhodococcus opacus* 0.3 g/L) it reach its critical micelle concentration (CMC). That is, the bacteria tends to form micelles instead of being adsorbed at the interface air-water, because the former configuration is more energetically favorable (Pashley *et al.*, 2004). In addition, Fig. 3-11 (b) shows that the surface tension of the bacterial suspension increases with the pH. Based on electrophoretic studies (Merma *et al.*, 2013, Botero *et al.*, 2008), *Rhodoccocus opacus* has an isoelectric point (IEP) around 3; therefore the bacteria may be more apolar at acid pH maximizing its hydrophobicity.

PUC-Rio - Certificação Digital Nº 1421964/CA

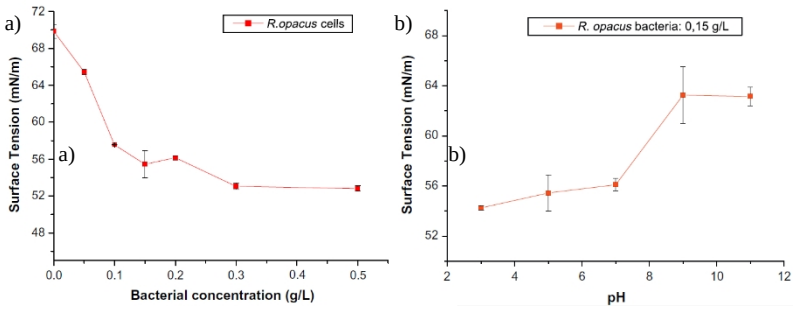

Figure 3-11: Surface tension of R. opacus as function of the biomass concentration (a) and pH (b) (Merma et al., 2013).

3.8.2. Surface charge

As it was discussed previously, *Rhodococcus opacus* is a hydrophobic bacteria, therefore it is expected its absence of superficial electric charge. In reality, it possesses a small surface potential that it is strongly dependent on the pH, as was demonstrated by electrophoretic studies (Merma *et al.*, 2013). Table 3-2 shows the IEP of *R. opacus* reported by several authors.

Table 3-2: Isoelectric point of *R. opacus* determined in several studies

IEP	Authors
2.0-2.8	Rijnaarts et al. 1995
3.0	Mesquita et al. 2003
3.2	Botero et al. 2008
2.8	Merma et al. 2013

FTIR studies identified carboxyl and amine groups (Botero *et al.*, 2008) which form part of proteins, amino acids, fat oils, nucleic acids and lipopolysaccharides. Fig. 3-12 shows the speciation of the carboxylic and amino groups in function of the pH for a generic amino acid. Bellow pH 2 the protonated form of both groups predominate ($NH3^+$ and COOH); at greater pH, the proportion of the deprotonated carboxylic group (COO^-) increases; finally at a pH around 9, the deprotonated amino group appears (NH_2). Therefore, in a pH range between 2 and 3, the bacteria may present a positive surface charge. On the other hand at pH greater than 3, begins to appear anionic species such as COO^- turning the surface negative.

PUC-Rio - Certificação Digital Nº 1421964/CA

In addition, there may be displacement of the mycolic acids found in the outer cellular wall, which would expose the peptidoglycan layer than contains ketone and ether groups that are highly nucleophilic (Mcmurry, 2012). These nucleophilic regions would attract species of opposite charge such as water dipoles, counter ions, hydroxyl groups, etc. Finally, it must take into account the inactivation process. Because of the autoclaving, some cells are going to suffer lysis, releasing intracellular compounds into the solution, some of these compounds may have a polar nature, which could explain the electric potential detected by the instrument.

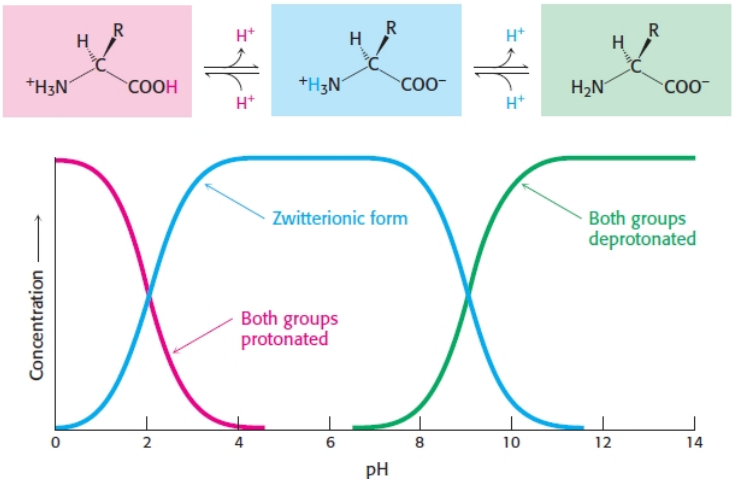

Figure 3-12: Speciation of amino and carboxylic groups as a function of pH. (Berg et al., 2012).

3.8.3. Electrokinetic studies

It was studied the electrokinetic behavior of the hematite and quartz before and after interaction with the bacteria *Rhodococcus opacus* (Mesquita *et al.*, 2003). The IEP for the mineral samples corresponded to pH values of approximately 2.0 for quartz and 5.1 for hematite. According to these results, it is possible to foresee a window in the pH range that is a potential region for electrostatic interaction between the mineral samples and the *R. opacus* cells. For quartz, this region was reported to exist at pH values below 3.5, and for hematite in the pH range of 3.2–5.5. In these regions the surface charge of the bacteria and minerals are opposite; so there exists an attractive force due to electrostatic interactions. After the interaction with the bacteria, the surface properties of both minerals changed as was evidenced by their different zeta potential profile. In addition, there was a displacement in the IEP, shifting from 5.1 to 2.6 in the case of hematite, and from

PUC-Rio - Certificação Digital Nº 1421964/CA

about 2.0 to 3.7 in the case of quartz (Mesquita et al. 2003). It should be noted, that the mineral surfaces turn hydrophobic as approach their IEPs. In the case of quartz, before bacterial interaction, it was not possible to determine its IEP in the pH range; however, after bacterial interaction the modified quartz surface reached an IEP of 3.7 (Merma et al. 2013). Fig. 3-13 shows the zeta potential of *R. opacus* cells, quartz and hematite as a function of pH, the size of mineral samples is lesser than 37 ⇑m.

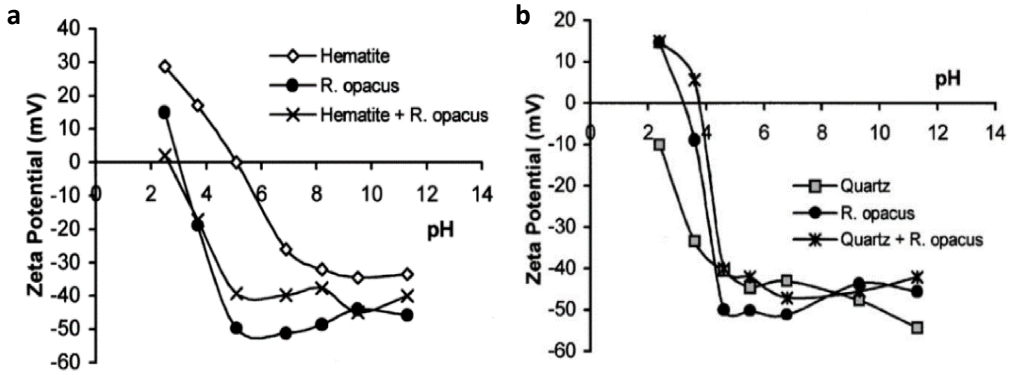

Figure 3-13: Zeta potential of R. opacus cells, quartz and hematite as a function of pH for hematite (a) and for quartz (b) before and after the interaction with cellular suspension (Mesquita et al., 2003).

3.8.4. Microflotation tests

Hematite flotation with *R. opacus* reported to have a significant recovery, around 90%, at pH 4, the floatability of the quartz is, however, considerably smaller than that of hematite (Mesquita *et al.*, 2003), Fig. 3-14. These results agree with the zeta potential and adhesion studies. For hematite, besides electrostatic interactions, chemical adsorption (hydrogen bonding, chemical interaction forces) may be involved in the bacterial–mineral interface (Van Loosdrecht *et al.*, 1989), resulting in a hydrophobic surface and a high floatability (about 70%) for pH values around 7.0.

PUC-Rio - Certificação Digital Nº 1421964/CA

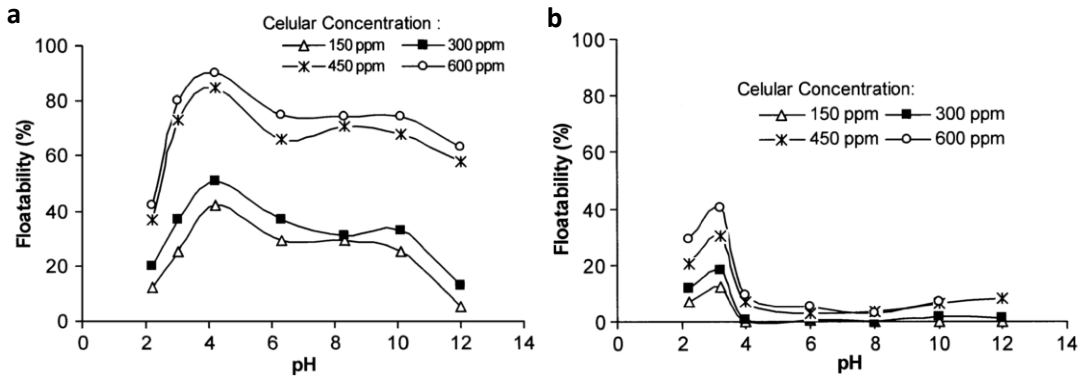

Figure 3-14: Floatability of hematite (a) and quartz (b) as function of R. opacus cells' concentration and pH (Mesquita et al., 2003).

3.9. Mineral flotation studies using biosurfactants as reagent

3.9.1. Modification of magnesite and serpentinite using biosurfactants

Zeta potential and isoelectric point measurement of magnesite and serpentinite particles before and after interaction with the biosurfactant contained om the broth solution were carried out (Didyk-Mucha *et al.*, 2015). An IEP shift from pH 4.5 to 2.0 was reported in the case of serpentinite suggesting that this biosurfactants is negatively charged and readily adsorbed onto the serpentinite surface, resulting in a new zeta potential profile. The assumption that the biosurfactant has an anionic nature is supported by the fact that cationic biosurfactants have been described extremely rarely, probably because they have a toxic effect, just like cationic surfactants in general (Hausmann *et al.*, 2015). Regarding to the magnesite, it suffered less modification by the biosurfactants compared with the serpentinite.

Significant selectivity was achieved after the activation with the biosurfactants between pH 6.6 and 7.2 as Fig. 3-15 shows, even though the recovery was low. The recovery after 30 min flotation for activated magnesite was up to 50%, while the recovery of activated serpentinite was only 35%. The flotation tests were conducted using a Hallimond tube.

PUC-Rio - Certificação Digital Nº 1421964/CA

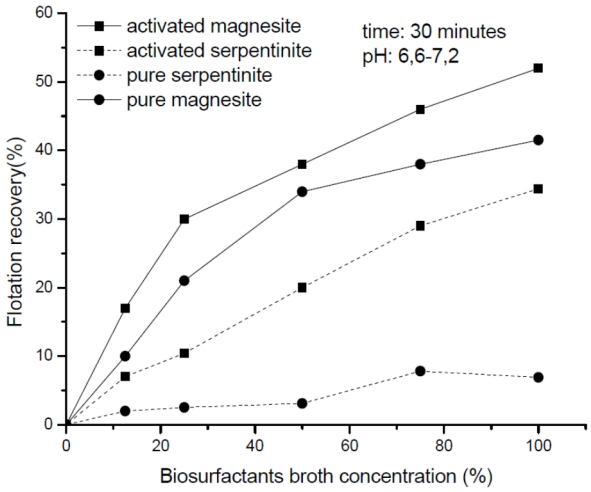

Figure 3-15: Magnesite and serpentenite bioflotation as a function of biosurfactant concentration (Didyk-Mucha et al., 2015).

3.9.2. Coal flotation using a biosurfactant from *Pseudomonas aeruginosa* as a frother

It was compared the biosurfactant capacity to low the water surface tension against a synthetic one, the MIBC (Methyl Isobutyl Carbinol). The biosurfactant showed good frothability in terms of reducing surface tension of water, froth height, and froth stability (Fazaelipoor *et al.*, 2010). By surface tension measurements, it was reported that the rhamnolipids showed more surface activity compared to the tested frothers commercially applied in mineral flotation industry (Khoshdast *et al.*, 2012). In addition, the froth stability produced by rhamnolipid was considerable better than the produced by the synthetic reagent (Khoshdast *et al.*, 2012).

3.9.3. Effects of biosurfactants on surface properties of hematite

It was studied hematite flotation with rhamnolipids produced by *Pseudomonas aerugiosa*, reporting an IEP shift of hematite towards higher pH values as the concentration of the biosurfactant increases (Szymanska et al. 2010). A similar phenomenon in the presence of bacteria cells in other study (Deo and Naratajan, 1997).

Flotability of hematite particles was examined in the presence of pure rhamnolipid and broth solution, Fig. 3-16. Hematite flotation was significantly

PUC-Rio - Certificação Digital Nº 1421964/CA

depressed by broth; this behavior would suggest a better affinity of organic metabolites from broth onto the hematite surface. On the other hand, significant increase in hematite floatability was observed at 20 ppm of pure rhamnolipid after 20 min. (Szymanska *et al.*, 2010).

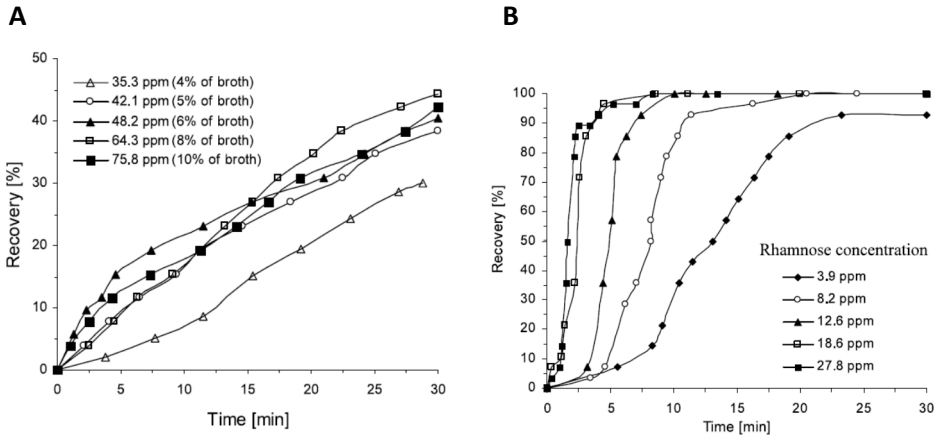

Figure 3-16: Hematite flotation with broth (A) and pure biosurfactant (B)(Szymanska et al., 2010).

Finally, these studies showed the potential use of biosurfactants in the mineral flotation industry. Even though, currently there are several obstacles to overcome such as their high processing cost and their low recovery (Szymanska *et al.*, 2010); optimization of the culture media, phenotype adaptation and genetic modification may be the solution to this problem, obtaining as a result an over producing biosurfactant microorganism (Mutalik *et al.*, 2008).

PUC-Rio - Certificação Digital Nº 1421964/CA